

Modulated phase matching and high-order harmonic enhancement mediated by the carrier-envelope phase

Daniele Faccio,^{1,2,*} Carles Serrat,^{1,3} José M. Cela,⁴ Albert Farrés,⁴ Paolo Di Trapani,^{2,5} and Jens Biegert^{1,6}

¹ICFO-Institut de Ciències Fotòniques, Mediterranean Technology Park, E-08860 Castelldefels, Barcelona, Spain

²CNISM and Department of Physics and Mathematics, Università dell'Insubria, Via Valleggio 11, I-22100 Como, Italy

³DTDI Universitat de Vic, Carrer de la Laura 13, E-08500 Vic, Barcelona, Spain

⁴CASE Barcelona Supercomputing Center, Carrer Gran Capità 2-4, E-08034 Barcelona, Spain

⁵Virtual Institute for Nonlinear Optics, Centro di Cultura Scientifica Alessandro Volta, Via Olmo Via Simone Cantoni 1, I-22100 Como, Italy

⁶ICREA Institució Catalana de Recerca i Estudis Avançats, E-08010 Barcelona, Spain

(Received 7 July 2009; revised manuscript received 10 November 2009; published 8 January 2010)

The process of high-order harmonic generation in gases is numerically investigated in the presence of a few-cycle pulsed-Bessel-beam pump, featuring a periodic modulation in the peak intensity due to large carrier-envelope-phase mismatch. A two-decade enhancement in the conversion efficiency is observed and interpreted as the consequence of a mechanism known as a nonlinearly induced modulation in the phase mismatch.

DOI: [10.1103/PhysRevA.81.011803](https://doi.org/10.1103/PhysRevA.81.011803)

PACS number(s): 42.65.Ky

Recent developments in ultrashort laser pulse technology have proved the viability and effectiveness of producing extreme ultraviolet (XUV) radiation by high-order harmonic generation (HHG) of ultrashort laser pulses in low-pressure gases. Both the phase of the driving laser field and phase accumulated during propagation will finally determine how the XUV field coherently builds up so that, in general, in order to achieve efficient HHG along a defined propagation direction phase, matching requirements must be fulfilled [3–5]. The propagation distance over which this occurs is defined as the coherence length $\ell_c = \pi/|\Delta K|$, where the total phase mismatch ΔK for HHG from the fundamental laser frequency ω to the q th harmonic may be written as

$$\Delta K = K_{\text{disp}} + K_{\text{plasma}} + K_{\text{atomic}} + K_{\text{geometric}}. \quad (1)$$

The contribution due to gas dispersion is $K_{\text{disp}} = qk_{\text{laser}} - k_q$, where k_{laser} and k_q are the laser and Harmonic pulse wave vectors, respectively. This term, which typically has a positive sign for gas pressures of, for example, <50 mbar, can be neglected [6]. The plasma dispersion term may be written as $K_{\text{plasma}} = \omega_p^2(1 - q^2)/2q\omega$, where ω_p is the plasma frequency, and gives a negative contribution [4], while the atomic dipole phase term K_{atomic} , related to the quantum paths of the electrons involved in the HHG process, in general does not have a fixed sign during propagation since it is proportional to the intensity gradient along the propagation direction, dI/dz [3,7]. Finally, the geometric term $K_{\text{geometric}}$ depends on the shape of the driving laser pulse. Unfortunately, the typical coherence lengths for conventional Gaussian laser pulses are $\ll 1$ mm, which severely limits the efficiency of the HHG process.

Tailoring of the $K_{\text{geometric}}$ term is one of the main approaches that have been considered for achieving phase matching in HHG. Specifically, truncated Bessel beams, obtained by refocusing with a lens the output of a hollow core waveguide, have been proposed and the specific phase profile, related to the geometry of the driving pulse, has shown to lead to improved

HHG brightness [8,9]. More recently, unfocused pulsed Bessel beams (PBBs) have also been considered [10,11]. PBBs have carrier wave vectors distributed over a conical surface so that the resulting interference pattern is characterized by a central intense peak with surrounding low-intensity rings [12]. By changing the angle γ of the wave-vector, cone it is possible to continuously tune the negative geometric term, $K_{\text{geometric}} = -q(\omega/c)(1 - \cos \gamma)$ [10], and thus achieve perfect phase matching ($\Delta K \simeq 0$) for a wide range of operating parameters. Due to the negative sign of this last contribution, phase-matching is possible only in the presence of a positive material dispersion (e.g., at high gas pressures) that is larger than the negative plasma contribution.

The second approach that has been demonstrated is the so-called quasi-phase-matching (QPM) technique. In this case the *amplitude* of the locally generated harmonic field is periodically damped at propagation distances corresponding to odd multiples of the coherence length ℓ_c [5,13–17]. In so doing, the remaining contributions add up coherently to the generated harmonic, whose average intensity keeps growing with propagation until absorption starts playing a dominant role.

In this article we draw attention toward a third phase-matching mechanism, which relies upon the occurrence of a periodic *phase modulation* imposed on the locally generated harmonic source. Specifically, we propose a technique to improve the efficiency of HHG with few-cycle pulses by controlling their carrier envelope phase (CEP) so as to achieve a periodic modulation of the pump peak intensity along with propagation. Owing to the inherent dependence of the harmonic phase on the pump intensity, a periodic acceleration/deceleration in the local contribution to the harmonic field is obtained, which results in an overall increase in the efficiency of the HHG process.

Control of the CEP requires control over both the phase velocity, which determines how the carrier-wave propagates, and the group velocity, which determines how the pulse envelope propagates. Our proposal is to achieve this by use of PBBs. We first note that the PBB is just a particular case of a larger family of “conical” pulses for which the wave vectors

*daniele.faccio@uninsubria.it

propagate along a cone with angle γ and a pulse front that, in general, may be tilted by an angle δ with respect to the wave vector. The carrier-wave velocity, v_ϕ , and the envelope velocity, v_p , along the propagation direction are related to the cone and tilt angles by [18]

$$v_\phi = \omega_L / (K_L \cos \gamma) \quad (2)$$

$$v_p = \cos \delta / K' \cos(\gamma + \delta), \quad (3)$$

where it is implied that the ω_L and K_L are the laser pulse carrier frequency and wave vector, respectively, and $K' = dK/d\omega$ is related only to material dispersion and is evaluated at ω_L . In general, we may thus independently choose the angles γ and δ so that the phase and peak velocities are effectively two independent and tunable quantities. We focus our attention on the specific case $\delta = -\gamma$, that is, the PBB, as this allows sufficient control over the phase and group velocity difference while remaining experimentally easy to generate by means of phase holograms [19,20] or ultrashort-pulse parametric amplification [21]. For the case of a PBB, Eq. (3) becomes $v_p = \cos \gamma / K'$. The difference between the phase and peak velocities will induce a beating in the pulse peak intensity with a periodicity that is twice that of the CEP and is a function of the cone angle γ ,

$$\Lambda(\gamma) = \frac{\pi}{\omega_L |v_\phi(\gamma)^{-1} - v_p(\gamma)^{-1}|}. \quad (4)$$

So, for example, for a Bessel cone angle $\gamma = 1$ deg, Eq. (4) predicts a periodicity in the pulse intensity modulation $\Lambda = 1.28$ mm.

In Fig. 1(a) we show a cross-section of the geometry of the PBB. The tilted wave fronts propagate at an angle with respect to the propagation direction, z . The region in which they overlap is called the Bessel zone (darker shaded area in the figure): the line corresponding to $z = 0$ indicates the position at which the PBB is considered in the present study as the input condition.

In order to verify the impact of such a pulse geometry on HHG, we performed numerical simulations based on a three-dimensional propagation model in cylindrical coordinates using the nonadiabatic strong-field approximation [22] to calculate the atomic response, as outlined in [6]. The computational code is fully parallelized with typical runs of 24 h using 256 CPU in a high-performance interprocess

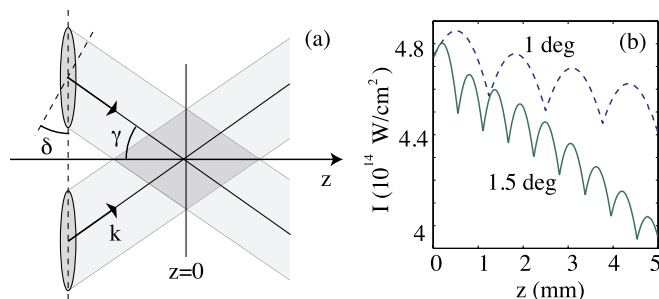


FIG. 1. (Color online) (a) Scheme of pulsed-Bessel-beam geometry. γ and δ are the Bessel cone angle and the pulse-front tilt angle, respectively. $z = 0$ indicates the position of the input condition for the numerical simulations. (b) Calculated peak intensity evolution along the z axis for the PBB for two different cone angles, $\gamma = 1, 1.5$ deg.

communication system. The laser pulse central wavelength was chosen to be 800 nm, and the input field was written as $E = E_0 J_0(r\omega_L \sin \gamma/c) \exp[-(r/\rho)^2] \exp[-(t/\tau)^2] \cos(\omega_L t)$ with a pulse duration at full width at half maximum (FWHM) of 5 fs (approximately two optical cycles). The Gaussian apodization in the transverse dimension was chosen to have a FWHM of 1.2 mm and the peak input intensity in all cases was 5×10^{14} W/cm². This corresponds, for example, to a total energy of 150 μ J for $\gamma = 1$ deg. HHG was performed in neon gas at a pressure of 20 mbar over a propagation distance of 5 mm. These values were chosen so as to have very weak reabsorption and thus observe the effect in the simplest case. In Fig. 1(b) we show the evolution along the propagation direction of the peak intensity of the PBB for two different cone angles. The CEP-induced oscillations are clearly visible in the figure with periodicities that correspond to Eq. (4). The slow decrease in the average intensity is due mainly to an effective negative second-order dispersion which arises due to the pulse front tilt in the PBB [18]. This negative dispersion at the pump pulse frequency may be partially compensated for by the positive material dispersion or eliminated by resorting to the use of more complicated nondispersive pulses known as X waves [18,23]. However, notwithstanding this slow intensity decrease, a clear enhancement in the XUV spectrum is observed, as shown in Fig. 2.

Three different cases are considered, $\gamma = 0.5, 1$, and 1.5 deg. The radially integrated spectral energy of the XUV radiation (in Joules) per photon energy unit (in eV) is shown in Fig. 2(a) for $\gamma = 0.5$ and 1.5 deg [the energies have been normalized to that of $\gamma = 0.5$ deg at the cutoff (116.2 eV) for clarity]. The 1.5 deg PBB shows a one-decade enhancement of the XUV intensity around 30 eV and the 0.5 deg PBB shows a nearly two-decade enhancement around 40–80 eV, with respect to that of a Gaussian pulse (solid line indicated as “0 deg”). Most interestingly, it is also clear how a change in the PBB cone angle shifts the phase-matched spectral region (with increasing photon energies for decreasing cone angles). Figure 2(b) shows

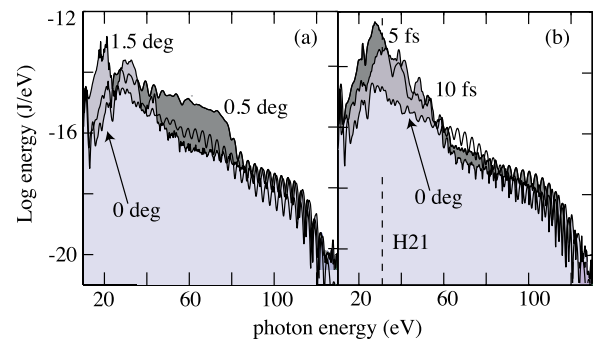


FIG. 2. (Color online) XUV relative spectral energy (in logarithmic scale) versus photon energy for three different PBB cone angles. (a) Dark shaded spectrum, 1.5 deg; light shaded spectrum, 0.5 deg. (b) 1 deg with two different pulse durations: dark shaded spectrum, 5 fs; light shaded spectrum, 10 fs. The thin black line indicated in both graphs with 0 deg is the reference spectrum obtained with a Gaussian pump pulse that has a FWHM of 40 μ m. The spectral energy for 1 and 1.5 deg has been normalized to that of 0.5 deg at the cutoff (116.2 eV).

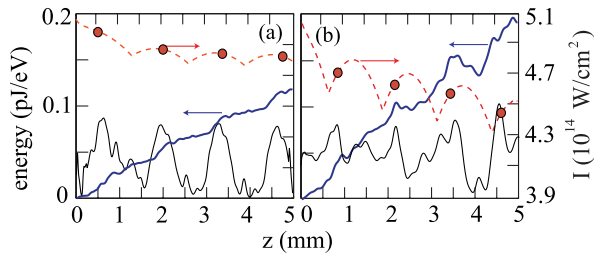


FIG. 3. (Color online) Thick solid lines, 21st harmonic energy for two different values of the input pulse duration: (a) 10 fs and (b) 5 fs. The dashed red lines show the laser pulse intensity (right axis) for the two cases. The thin solid lines show the derivative with respect to z of the harmonic energies.

the XUV spectra for $\gamma = 1$ deg and for two different pulse durations, 10 and 5 fs. The enhancement obtained with the 10-fs pulse lies somewhere between the 5-fs and the Gaussian-pulse spectrum. This is a result of the decrease in the intensity modulation depth that decreases to zero with increasing pulse duration.

In Fig. 3 we examine the XUV signal propagation in more detail. In particular, we study the dependence of the 21st harmonic on the CEP oscillations for a PBB with $\gamma = 1$ deg and a pulse duration of 10 fs in Fig. 3(a) and 5 fs in Fig. 3(b). In both cases, the harmonic (thick solid line) is seen to increase nearly monotonically in contrast to the harmonics (e.g., H41) in the nonenhanced regions that exhibit fast fluctuations around an average, constant value (data not shown). If we take the derivative with respect to z of the harmonic energy (thin solid lines), we clearly see a series of peaks. These peaks, representing maximum XUV energy increase, occur with the same periodicity of the CEP oscillations (see the solid circles in the figure), which demonstrate the key role played by the CEP modulation in the XUV energy growth. However, as shown in Fig. 3(b), the peak positions do not necessarily coincide with those ones where the laser-pulse intensity is maximum. Moreover, the average harmonic energy shows a virtually linear dependence on the propagation distance, in contrast with the quadratic power law which typically features a QPM regime. These results hinder the possibility of interpreting the observed phenomenon as a standard QPM. Note that here CEP periodicity is in the mm range while ℓ_c is typically in the 100- μm range (discussed later in this article), implying a high QPM order and a consequently reduced QPM efficiency that is difficult to associate with the large enhancement shown in Fig. 2.

In order to ascertain which is the dominant mechanism responsible for the results in Fig. 2, we remark that the harmonic field at a given propagation distance z results from the sum of the propagated (free term) and of the locally generated (forced term) fields. The considerations mentioned earlier in this article indicate that the periodic increase in the XUV signal cannot be simply ascribed to a periodic *amplitude* modulation of the forced term, as for the usual QPM. On the contrary, we propose that the enhancement is related to a periodic modulation in the forced-term *phase*. To this end let's consider in more detail Eq. (1). As already pointed out, in our operating conditions we may neglect the first (material dispersion) term. The geometric term due to the

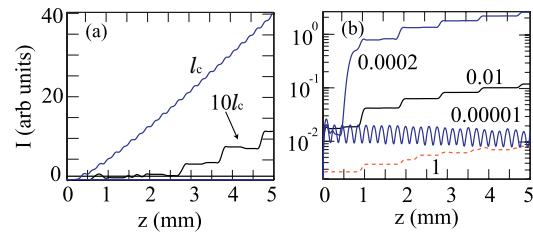


FIG. 4. (Color online) A generic harmonic intensity evolution versus z in the presence of periodic phase modulation. (a) Modulation depth $\epsilon = 0.0001$, different values of the phase modulation periodicity $\bar{\Lambda}$ are indicated in the graph. (b) For a fixed $\bar{\Lambda} = 10\ell_c$, the modulation depth ϵ is varied as indicated in the graph.

Bessel pulse geometry is $\sim 2.5 \times 10^4 \text{ m}^{-1}$, while the plasma term is an order of magnitude smaller and may thus, to a first approximation, be neglected. If we now consider a PBB with oscillating intensity, we see that the atomic dipole term ($\propto dI/dz$) will also oscillate and may become important. As a consequence, the phase of the forced oscillator is periodically delayed and accelerated, becoming locally closer to that of the free term. In other words, the phase mismatch is periodically modulated as a consequence of modulation of the pump. The resulting breaking of the symmetry between in- and out-of-phase contributions can justify an overall growth in the harmonic field. We have directly verified this conjecture by considering a generic harmonic signal, E , which propagates linearly in a dispersive medium and at each propagation step added to a modulated, forced, harmonic contribution, according to $E_n = E_{n-1} \exp[ik_q(z_n - z_{n-1})] + \exp[iqk_{\text{laser}}(1 - \epsilon + |\epsilon \cos(\pi z_n / \bar{\Lambda})|)z_n]$, where ϵ is the modulation depth and the step $z_n - z_{n-1}$ is chosen small enough to resolve the phase-mismatch oscillations in the nonmodulated ($\epsilon = 0$) case. Figure 4(a) shows the resulting harmonic growth assuming a linear phase mismatch for the nonmodulated case $\Delta K_{\text{lin}} = qk_{\text{laser}} - k_q = 3.3 \times 10^4 \text{ m}^{-1}$. The optimal case is obtained when the phase modulation periodicity equals the coherence length, $\bar{\Lambda} = \ell_c$. The harmonic grows linearly and after 5 mm reaches a value roughly two orders of magnitude higher than the nonmodulated, phase-mismatched case (indicated by the horizontal line). The interesting feature of this new kind of phase-matching process is that even for $\bar{\Lambda} \gg \ell_c$ (e.g., $10\ell_c$), harmonic enhancement is still observed. Figure 4(b) shows the effect of changing the modulation depth, ϵ , as indicated in the figure, for a fixed $\bar{\Lambda} = 10\ell_c$. As the modulation depth decreases, the harmonic conversion actually increases reaching its maximum for $\epsilon = \epsilon_{\text{min}}$, while for $\epsilon < \epsilon_{\text{min}}$ the conversion decreases again. As we have verified, the largest conversion is obtained when exact phase matching is reached, without being surpassed (i.e., for $qk_{\text{laser}}|\epsilon_{\text{min}}| = \Delta K_{\text{lin}}$). For example, if we consider the parameters of Fig. 4(b), this condition is verified for $\epsilon = 0.0002$. Moreover, the z_n values for which the phase matching is verified corresponds to the points of maximum harmonic growth, thus explaining the steplike dependence versus z . The results in Fig. 4 are consistent with all the main features observed in our HHG simulations, that is, significant HHG enhancement: (i) with a steplike periodic dependence versus z , which is not necessarily in phase with the pump modulation; (ii) with a CEP modulation that is much larger than ℓ_c and is not a given multiple of ℓ_c ; (iii) with a relatively

weak CEP modulation depth; (iv) with an average growth rate that is linear in z .

In conclusion, we report a frequency conversion technique by which HHG may be enhanced in a tunable XUV spectral region. Due to the specific nature of the HHG process the pump intensity modulation translates into a phase modulation of the harmonic. The resulting modulation in the phase mismatch enhances the HHG process with a nearly two-decade increase in the XUV intensity with respect to a nonmodulated Gaussian pulse. The underlying mechanism is very general and may be applied to any nonlinear frequency conversion process, for example, second or third harmonic generation, provided that a method is found to impart a periodic phase modulation onto either the pump or the harmonic pulse. In analogy with the case of random phase matching, and differently from the cases of standard phase matching and QPM, the average harmonic

signal is found to grow linearly in propagation. Finally, in this work the main role is played by periodic on-axis intensity variations through the harmonic phase dependence on dI/dz . However, in general, there may also be a radial dependence dI/dr of the atomic dipole phase that may be tuned in order to further optimize harmonic growth.

The authors acknowledge support from the Consorzio Nazionale Inter-universitario per le Scienze della Materia (CNISM), progetto INNESCO. J.B. and C.S. acknowledge support from the Spanish Ministry of Education and Science through its Consolider Program Science (SAUUL-CSD 2007-00013), as well as through Plan Nacional (FIS2008-06368-C02-01/02). Computer resources and assistance provided by the Barcelona Supercomputing Center is acknowledged.

-
- [1] K. J. Schafer, B. Yang, L. F. DiMauro, and K. C. Kulander, *Phys. Rev. Lett.* **70**, 1599 (1993).
- [2] P. B. Corkum, *Phys. Rev. Lett.* **71**, 1994 (1993).
- [3] P. Balcou *et al.*, *Phys. Rev. A* **55**, 3204 (1997).
- [4] T. Pfeifer *et al.*, *Rep. Prog. Phys.* **69**, 443 (2006).
- [5] A. Paul *et al.*, *IEEE J. Quantum Electron.* **42**, 14 (2006).
- [6] E. Priori *et al.*, *Phys. Rev. A* **61**, 063801 (2000).
- [7] M. Lewenstein, P. Salieres, and A. L'Huillier, *Phys. Rev. A* **52**, 4747 (1995).
- [8] M. Nisoli *et al.*, *Phys. Rev. Lett.* **88**, 033902 (2002).
- [9] C. Altucci *et al.*, *Phys. Rev. A* **68**, 033806 (2003).
- [10] A. Averchi *et al.*, *Phys. Rev. A* **77**, 021802(R) (2008).
- [11] T. Auguste, O. Gobert, and B. Carre, *Phys. Rev. A* **78**, 033411 (2008).
- [12] A precise definition of the PBB requires that the cone angle, γ , varies with frequency such that the transverse wave vector, $k_{\perp} = (\omega/c) \sin \gamma(\omega)$, is constant. In the text, γ is to be understood as the cone angle at the carrier frequency of the pulse.
- [13] A. Paul *et al.*, *Nature (London)* **421**, 51 (2003).
- [14] E. A. Gibson *et al.*, *Science* **302**, 95 (2003).
- [15] O. Cohen *et al.*, *Phys. Rev. Lett.* **99**, 053902 (2007).
- [16] A. Pirri, C. Corsi, and M. Bellini, *Phys. Rev. A* **78**, 011801(R) (2008).
- [17] X. Zhang *et al.*, *Nat. Phys.* **3**, 270 (2007).
- [18] M. Porras, G. Valiulis, and P. DiTrapani, *Phys. Rev. E* **68**, 016613 (2003).
- [19] J. Dyson, *Proc. R. Soc. London, Sect. A* **248**, 93 (1958).
- [20] J. Sochacki *et al.*, *Appl. Opt.* **31**, 5326 (1992).
- [21] M. Clerici *et al.*, *Opt. Lett.* **33**, 2296 (2008).
- [22] M. Lewenstein, P. Balcou, M. Y. Ivanov, A. L'Huillier, and P. B. Corkum, *Phys. Rev. A* **49**, 2117 (1994).
- [23] E. Recami, *Phys. A* **252**, 586 (1998).